Crystallization and Melting Behaviors of Maleated Polyethylene and Its Composite with Fibrous Cellulose

Farao Zhang, Wulin Qiu, Liqun Yang, Takashi Endo, Takahiro Hirotsu

Institute for Marine Resources and Environment Research, National Institute of Advanced Industrial Science and Technology, 2217-14 Hayashi-Cho, Takamatsu 761-0395, Japan

Received 26 November 2001; accepted 11 December 2002

ABSTRACT: The crystallization and melting behaviors of maleated polyethylene (MPE) and its composite with fibrous crystalline cellulose are investigated by differential scanning calorimetry. MPE exhibits a higher crystallization starting temperature, because of the interactions between maleic anhydride (MA) groups for nucleation, and lower melting and crystallization enthalpies, because of the intensive irregularity of MPE chains compared to unmaleated PE (UPE). Fibrous cellulose (FC) slightly facilitates the nucleation of MPE but causes no change in the transition enthalpies of MPE for crystallization and melting in UPE–FC and MPE–FC composites. The kinetics of crystallization show that the Avrami exponent depends on the content of MA groups and FC to a small extent and the activation energy is largely determined by the MA content, suggesting the irregularity and decreased mobility of MPE chains that is due to the interactions between the grafted MA groups in MPE and the FC composite. © 2003 Wiley Periodicals, Inc. J Appl Polym Sci 89: 3292–3300, 2003

Key words: polyethylene; crystallization; composites; differential scanning calorimetry; polysaccharides

INTRODUCTION

Much attention has been directed to the development of cellulose–polyethylene (PE) composites from the viewpoint of extensive utilization of cellulose resources, as well as protection of the environment from waste plastics.[1] Although cellulose is the most abundant natural polymer on the earth, its application has been essentially limited to only a few areas such as paper and rayon because of its lack of thermoplasticity. The limitations on petroleum resources, however, will not permit the indefinite extensive utilization of oil-derived plastics. Thus, we have made efforts to develop novel cellulose compounds with a small amount of PE, which exhibit good mechanical properties and processability.[2,3]

Good adhesion between cellulose and PE is the key to realizing a composite of them with good mechanical properties. The most effective method to date for obtaining such adhesion is to use PE grafted with maleic anhydride (MA), which increases the compatibility of the PE matrix with cellulose through the esterification between the MA groups of maleated PE (MPE) and the hydroxyl groups of cellulose.[4–7] Many studies have been conducted on the chemical modification of PE with MA[8–10] and the structural characteristics of grafted MA groups.[11–13] However, little attention has been paid to the crystallization and melting behaviors of MPE, which are very important for an understanding of the morphology of the resulting MPE compound with cellulose.

Only a few studies have been reported on the crystallization behaviors of maleated polypropylene (MPP) and its salts with metal ions.[14–16] The introduction of MA groups to PP chains increases the crystallization rate, but it does not affect the crystallization mode. By contrast, natural cellulose favors nucleation of PP, producing a transcrystalline region around the cellulose fiber whereas surface treatment of the cellulose with alkyl ketene dimer or alkenyl succinic anhydride results in a nonnucleating surface and no transcrystallinity.[17] A previous study on a PP–chlorella blend indicated that the interaction between MPP and chlorella causes a decrease in the crystallinity of the MPP matrix, although unmaleated PP (UPP) exhibits no change in crystallinity because of the absence of such an interaction.[18] The effect of cellulose on the crystallization of MPE still remains unclear. A recent study on the mechanochemical preparation of a cellulose–PE composite has demonstrated that the MPE chains bonded on the cellulose particles are almost all in an amorphous state and cause a decrease in the crystallinity of MPE.[3]

We prepared fibrous cellulose (FC)–MPE composites by melt mixing FC with MPEs having different MA contents.[2] An FC with a high crystallinity exhibits almost no reactivity to MPE, which is quite different from the case in an amorphous state resulting from ball milling.[3] In this study, to understand the mor-

Correspondence to: T. Hirotsu (takahiro-hirotsu@aist.go.jp).

Journal of Applied Polymer Science, Vol. 89, 3292–3300 (2003)

phology of the FC–MPE composite and obtain the necessary information for processing of the composite, we investigate the effects of grafted MA and crystalline cellulose fiber on the crystallization of MPE and further explore the crystallization kinetics of MPE and its composite with FC.

EXPERIMENTAL

Material preparation

A commercially available grade PE (7000F grade, Mitsui Sekiyu Kagaku) was used for preparing MPE. The MPE samples were obtained by melt mixing PE with MA under conditions similar to those in a previous study.[2] The MA content in the MPE was determined by chemical titration. Four MPEs with 0.23, 0.47, 0.85, and 1.68 wt % MA (MPE_x, where x = 0.23, 0.47, 0.85, and 1.68) were used in this study. The average chain length of the grafted MA groups in MPE_x is in the following order: $MPE_{1.68} > MPE_{0.85} > MPE_{0.47} > MPE_{0.23} \approx 1$ MA unit.[2] The unmaleated PE (UPE) was also prepared by the same process as MPE without the addition of MA for comparison.

An FC (Whatman Int. Ltd.) with a crystallinity of 93% and average dimensions of approximately a 300-μm length and a 20-μm diameter[2,19] was used for preparing UPE–FC and MPE–FC composites. These composites were prepared by the same method as in our previous study.[2]

Test specimens for differential scanning calorimetry (DSC) measurements were obtained by cutting compression-molded sheets of UPE, MPE, and their composites. To achieve a homogeneous shape and approximate equal weight, all of the specimens were cut into disks of approximately 0.6-mm thickness to fit the sample pan.

DSC measurements

The DSC measurements were performed on a Perkin–Elmer Pyris 1 differential scanning calorimeter. Each sample was first heated to 210°C and kept at this temperature for 2 min to erase the thermal history. The sample was cooled to 50°C at a fixed rate, kept at that temperature for 2 min, and then heated again to 210°C at the same rate to finish the successive melting process. One cycle of nonisothermal crystallization and melting includes the processes described above. The thermal behaviors (temperature and enthalpy of crystallization and melting) were examined based on the data with a rate of 10°C/min. For the crystallization kinetics, five cycles of nonisothermal crystallization and melting were measured at different cooling and heating rates of 20, 15, 10, 5, and 1°C/min.

Kinetics of crystallization

Theory

Two processes of crystallization (isothermal and nonisothermal) have been considered to investigate the crystallization behaviors of polymers. For the isothermal crystallization, the Avrami equation[20,21] has been proposed as in eq. (1):

$$\alpha = 1 - \exp(-kt^n) \tag{1}$$

where n is the Avrami exponent, k is the rate constant, and α is the extent of crystallization at time t. The n value is dependent on the dimension of crystal growth and the nucleating mode. The k value is temperature dependent and may be expressed by the Arrhenius equation:

$$k = A\exp(-E/RT) \tag{2}$$

where A is a constant, E is the activation energy of crystallization, T is the crystallization temperature, and R is the gas constant.

From an isothermal DSC curve, k and n can be obtained as the intercept ($\ln k$) and slope (n) of the following equation, which is derived from eq. (1):

$$\ln[-\ln(1 - \alpha)] = n \ln t + \ln k \tag{3}$$

However, quick attainment of the starting temperature of isothermal crystallization is often difficult because the rapid change to the crystallization temperature leads to significant fluctuation of the background that is due to heat flow, which may cause partial crystallization before recovery of the stable baseline. Accordingly, this is quite unsuitable for polymers with rapid crystallization such as PE.

Only a few methods have been developed for the examination of the kinetics of nonisothermal crystallization of polymers,[22–24] and these methods are not convenient enough for analysis of the nonisothermal data.[25] Gupta et al.[26] proposed a direct method based on eq. (4), which is derived by differentiating eq. (1) twice with $d^2\alpha_p/dt_p^2 = 0$, assuming that E in eq. (1) is constant during the nonisothermal process.

$$[\alpha_p'(T_p - T_0)]/[\beta(1 - \alpha_p)] = (n - 1) + [E(T_p - T_0)]/(RT_p^2) \tag{4}$$

where T_0 is the starting temperature; T_p is the temperature corresponding to the peak of the nonisothermal exotherm; β is the cooling rate; α_p is the extent of crystallization at T_p, which is determined as the fractional area of the crystallization exotherm between T_0 and T_p to the total area of the exotherm; and α_p' is the

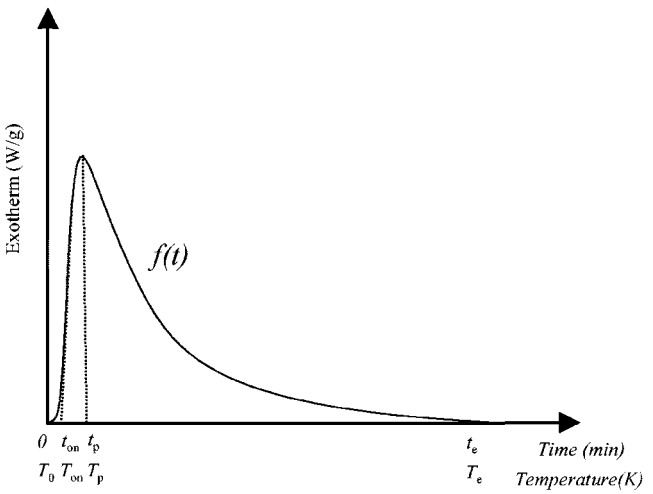

Figure 1 A sketch of a typical DSC curve of nonisothermal crystallization $f(t)$, where crystallization starts at time 0 (temperature T_0) and terminates at the end time t_e (temperature T_e), exhibiting the maximal at peak time t_p (temperature T_p).

derivative of α at T_p. The n and E constants in nonisothermal crystallization are obtained from eq. (4).

In this study, we measured the DSC curves of nonisothermal crystallization and analyzed the kinetics of crystallization based on eq. (4).

Determination of parameters

We describe the determination of the starting temperature, as well as the calculation of α_p and α_p', in this study because Gupta et al. did not show them clearly.[26] Figure 1 shows a typical DSC crystallization curve $f(t)$, where crystallization starts at time 0 (temperature T_0) and terminates at time t_e, exhibiting the maximal at time t_p (temperature T_p). Based on the definition described above, α_p is expressed as the following:

$$\alpha_p = \frac{\int_0^{t_p} f(t)dt}{S_e} \quad (5)$$

where

$$S_e = \int_0^{t_e} f(t)dt$$

Accordingly, α_p' is expressed by eq. (6):

$$\alpha_p' = \frac{f(t_p)}{S_e} \quad (6)$$

We can obtain the values of α_p and α_p' by analyzing the nonisothermal DSC curve with eqs. (5) and (6), respectively.

A problem arises from the determination of the starting temperature on a DSC crystallization curve. Most studies of crystallization kinetics have adopted the onset temperature (T_{on}) as the starting temperature, defined as the temperature at the point of the steepest tangent on an exotherm on the higher temperature side intersecting the baseline (see Fig. 1). However, the onset temperature does not necessarily reflect the real initiation of crystallization, because the exotherm has already occurred above T_{on} (Fig. 1). The adoption of T_{on} as the starting temperature probably introduces some inaccuracy, particularly in analyzing the kinetics of crystallization through a heterogeneous nucleation. Hence, we selected the point at which the exotherm curve just begins to deviate from the baseline as the starting temperature T_0. We determined T_0 from a deviation of 0.01 W/g from the baseline and hereafter call this temperature the trigger temperature of crystallization.

RESULTS AND DISCUSSION

Thermal behavior

Figure 2(a) shows DSC curves of crystallization for UPE and MPE_x (x = 0.23, 0.47, 0.85, and 1.68) and their composites with 30 wt % FC (70UPE–30FC, 70MPE_x–30FC). UPE exhibits a sharp exothermic peak, regardless of the compounding with FC. In contrast with UPE, MPE_x exhibits a broader exothermal peak, the broadness of which increases with x and increases further by compounding with FC. Their DSC curves of melting following crystallization are shown in Figure 2(b). The melting endotherms have profiles similar to the crystallization exotherms with respect to broadness. These results indicate that not only the existence of MA groups in MPE but also the compounding with FC have remarkable effects on the crystallization and melting of MPE.

Effect of MA groups in MPE

The crystallization and melting temperatures of MPE are shown against the MA content in Figure 3. The melting temperature decreases with an increase in the MA content. Conversely, the crystallization temperature increases with the content of MA groups. The most interesting feature is that the crystallization onset temperature of MPE is higher than the melting onset temperature. It is well worth noting that the difference in onset temperature between crystallization and melting becomes greater with an increase in the MA content. This implies strong interactions between MPE molecular chains that may induce the

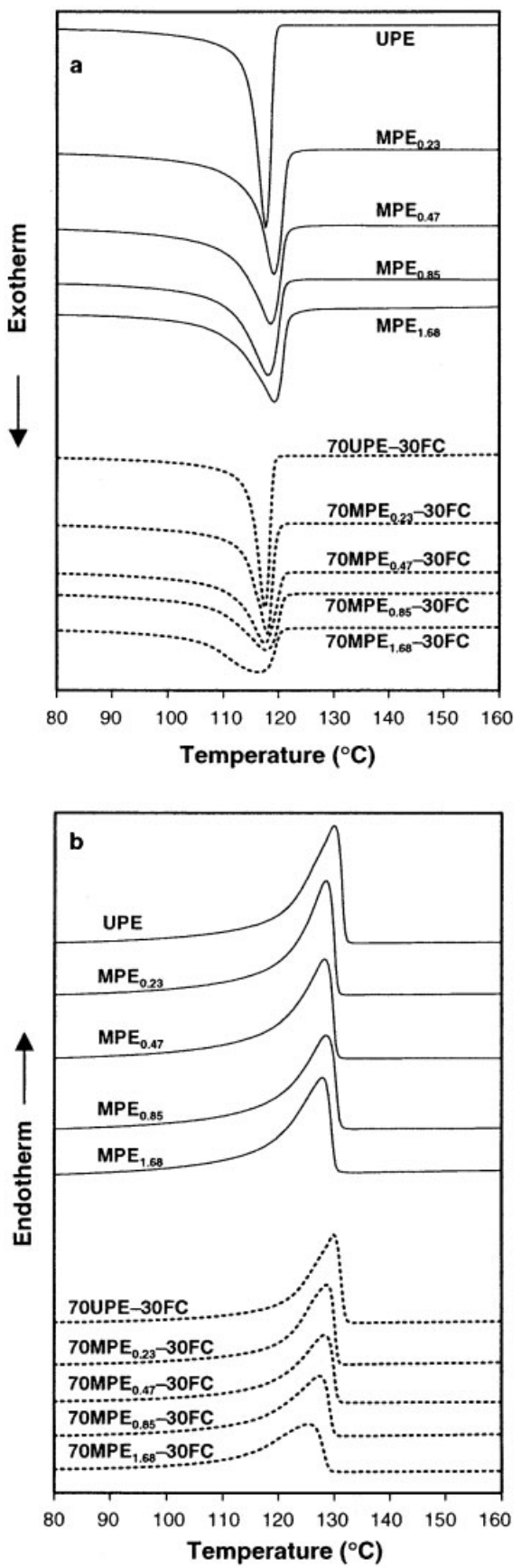

Figure 2 DSC thermograms of (a) crystallization and (b) melting of (—) UPE and MPE with different MA contents and (- - -) their composites with 30 wt % FC. The cooling and heating rates are 10°C/min.

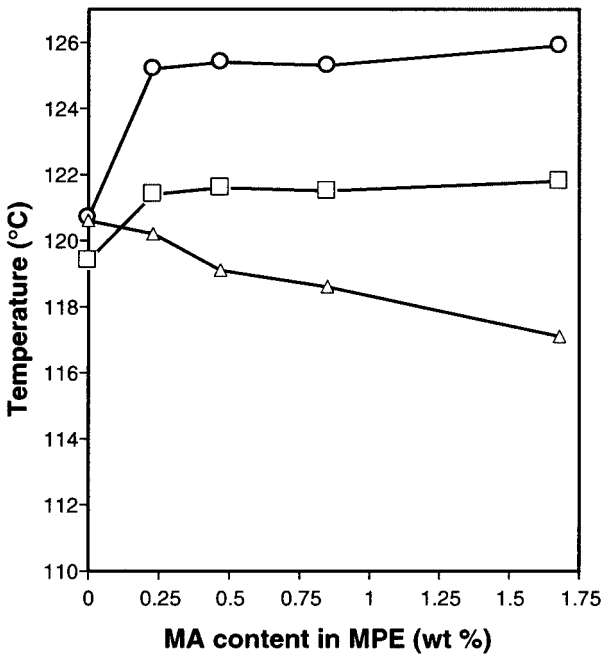

Figure 3 The effects of the MA content in MPE on the (○) crystallization trigger, (□) crystallization onset, and (△) melting onset temperatures.

nucleation of MPE, because crystallization generally occurs below the melting temperature as in the case of the UPE in Figure 3. The temperature difference in crystallization between trigger and onset, which is enlarged by the MA groups in MPE, implies that the nucleation mode induced by MA groups is probably heterogeneous. The enthalpies for both crystallization and melting of MPE decrease gradually as the MA content increases, as shown in Figure 4. The decreases in enthalpy are probably attributable to the lower crystallinity of MPE than PE.

Effect of FC in composite

The crystallization and melting temperatures of UPE–FC and $MPE_{0.47}$–FC composites are shown versus the FC content in Figure 5. The compounding of UPE with FC results in little change in the crystallization and melting temperatures from those for UPE. This reveals that FC acts only minimally as a nucleator for PE in the UPE–FC composites, unlike the case in the PP–FC composite.[17] On the other hand, the compounding of $MPE_{0.47}$ with FC results in a sharp drop in the trigger temperature of crystallization and a slight decrease in the onset temperature of melting at an FC content of 5 wt %, beyond which the tempera-

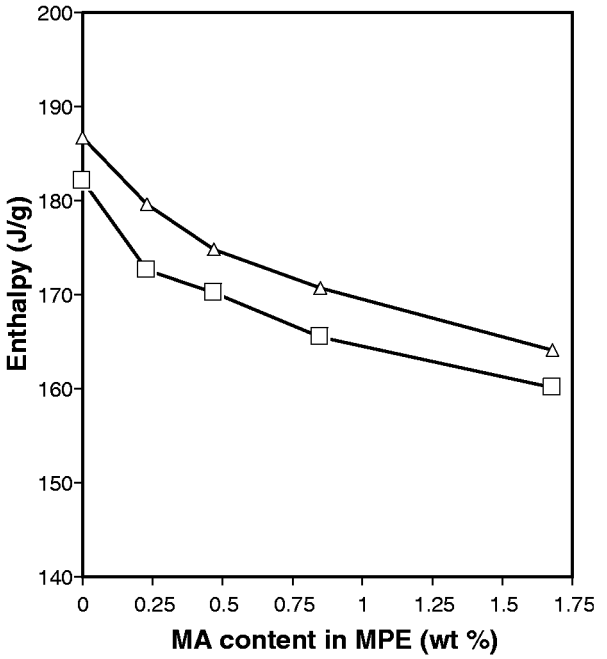

Figure 4 The effects of the MA content in MPE on the (□) crystallization and (△) melting enthalpies of MPE.

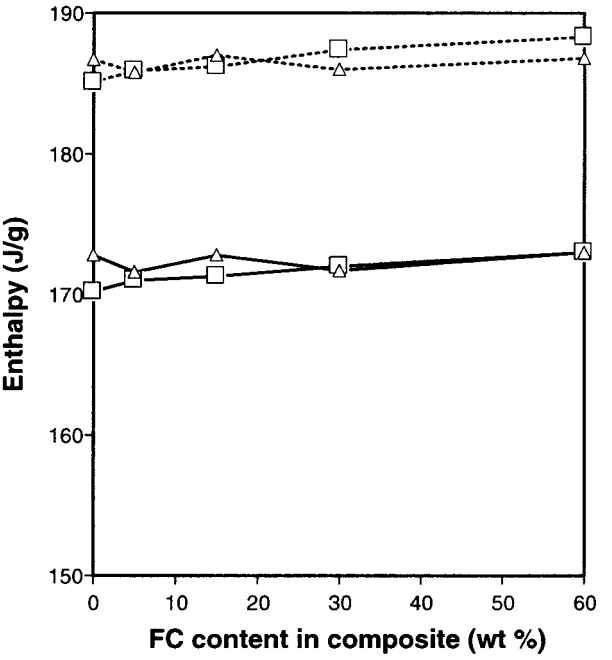

Figure 6 The effects of the FC content in the composite on the (□) crystallization and (△) melting enthalpies of (- - -) UPE–FC and (—) $MPE_{0.47}$–FC composites.

tures scarcely vary at all. These results indicate the occurrence of interactions between MPE and FC, possibly due to electrostatic attraction and/or hydrogen bonds rather than the formation of ester bonds between the MA groups of MPE and the OH groups of FC.[2] The large drop in the trigger temperature of crystallization suggests that the strong interaction between MPE and FC prevents the formation of the interactions between MPE chains necessary for the initiation of crystallization of MPE.

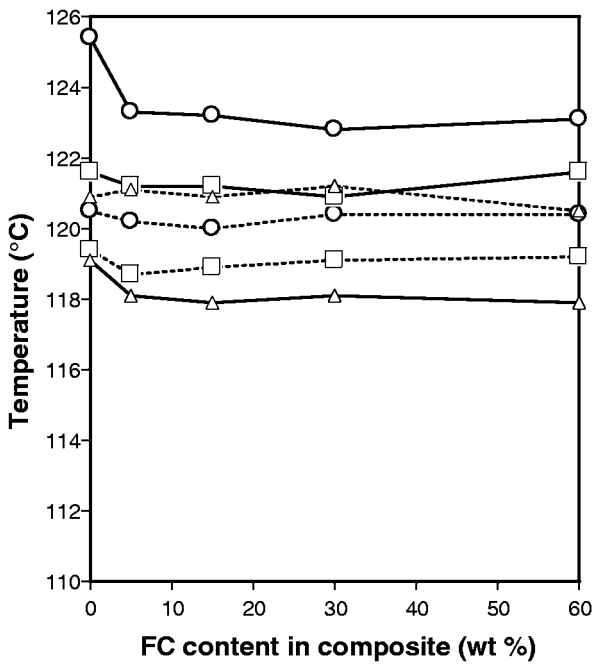

Figure 5 The effects of the FC content in the composite on the (○) crystallization trigger, (□) crystallization onset, and (△) melting onset temperatures of (- - -) UPE–FC and (—) $MPE_{0.47}$–FC composites.

The enthalpies for crystallization and melting of UPE–FC and $MPE_{0.47}$–FC composites are shown against the FC content in Figure 6. It is clear that the crystallization and melting enthalpies of UPE–FC and $MPE_{0.47}$–FC hardly change with the content of FC. Accordingly, the interactions between MPE and FC are so weak that the crystallinity of the MPE matrix is almost constant, regardless of the FC content. The FC used in this study is a kind of fibrous powder with a large particle size (>100 μm) and high crystallinity,[2,24] both of which are unfavorable for the formation of ester bonds with MPE.[2]

Kinetics of crystallization

DSC curves at different cooling rates

The kinetics of crystallization of UPE, MPE, and their compounds with FC were examined based on the nonisothermal DSC exotherms at different cooling rates. Figure 7 shows crystallization exotherms for UPE and $MPE_{0.85}$ and their composites with 15 wt % FC. Each DSC curve at a lower cooling rate has a higher trigger temperature of crystallization and a smaller apparent peak area. Note that the real crystallization enthalpy is not based on the apparent area but

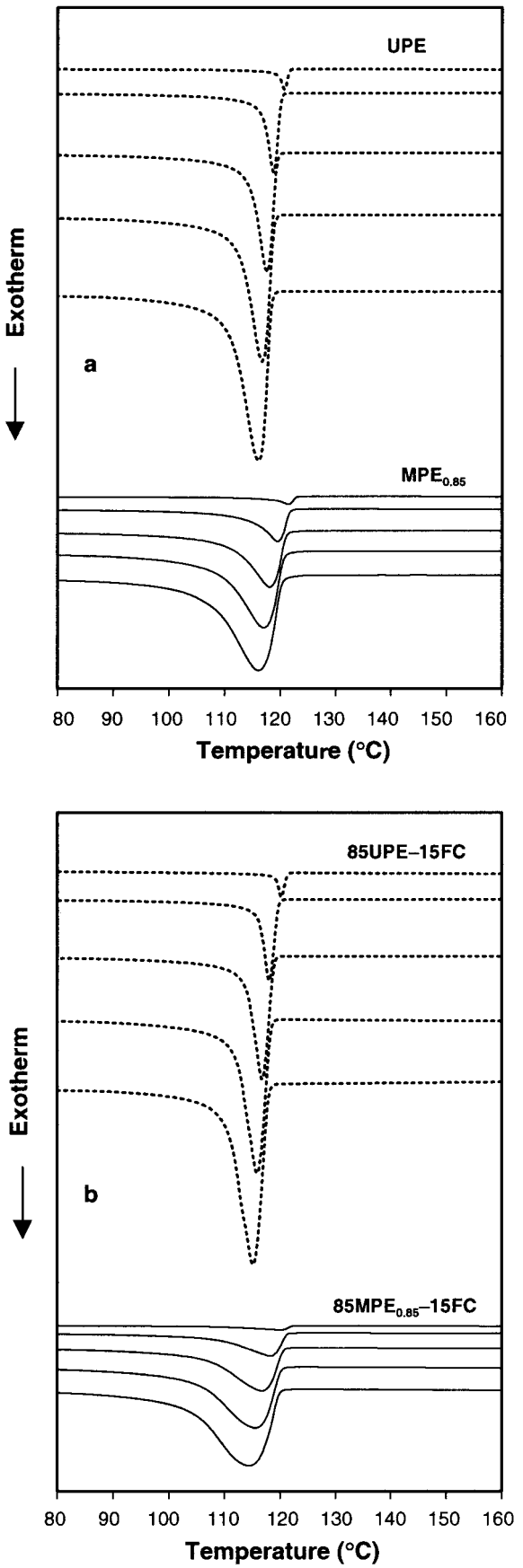

on the integration of heat flow over the whole time spent on crystallization.

Avrami exponent and activation energy

The parameters α_p and α_p' calculated according to eqs. (5) and (6) are listed for UPE and MPE in Table I and for their composites with 15 wt % FC in Table II. Plots of $[\alpha_p'(T_p - T_0)]/[\beta(1 - \alpha_p)]$ versus $[(T_p - T_0)/T_p^2]$ are shown for UPE and MPE in Figure 8(a) and for their composites with 15 wt % FC in Figure 8(b). These plots yield good linear relationships between $[\alpha_p'(T_p - T_0)]/[\beta(1 - \alpha_p)]$ and $[(T_p - T_0)/T_p^2]$, which make possible the calculation of the Avrami exponent and activation energy according to eq. (4). Thus, the values of n and E for UPE and MPE and their composites are shown versus the MA content in Figure 9(a,b), respectively. The Avrami exponent decreases with an increase of MA content in MPE, whereas the activation energy increases with the content of MA. The UPE–FC composite exhibits hardly any change in n with the FC content; but the MPE–FC composite demonstrates an obvious decrease in n at an FC content of 5 wt %, beyond which it remains almost unchanged. The UPE–FC and MPE–FC composites have almost the same E values as UPE and MPE, respectively.

The n values obtained for UPE and MPE and their composites are not integers, similar to those reported in the literature,[14,26,28] indicating that the crystallization processes are composed of complicated modes of nucleation and crystal growth. The n values in our study are smaller than those in the literature,[26,29,30] because our values are the averages of the whole temperature range of crystallization from T_0 to T_e. From eqs. (1) and (6) the smaller n value means the temperature range of crystallization is greater. Figures 2(a) and 9(a) demonstrate that MPE exhibits a broader exothermal peak with a decrease in the value of n.

The activation energy for crystallization consists of two parts: nucleation ($E_{\text{nucleation}}$) and crystal growth (E_{growth}). The $E_{\text{nucleation}}$ value of MPE is probably smaller than that of UPE, because polar MA groups on MPE chains induce intensive nucleation through strong interactions between MA groups, as shown in Figure 3. On the other hand, interactions between MA groups on MPE chains may make difficult the movement of the MPE chains to the surfaces of the crystals of MPE; furthermore, the folding of an MPE chain is also restricted to the length between two neighboring MA groups along with the chain. Accordingly, the

Figure 7 DSC curves of the (a) crystallization exotherm of (- - -) UPE and (—) $MPE_{0.85}$ and (b) (- - -) 85UPE–15FC and (—) $85MPE_{0.85}$–15FC composites at different cooling rates (1, 5, 10, 15, and 20°C/min, corresponding to the curves from top to bottom).

TABLE I
Characteristics of DSC Crystallization Exotherms of UPE and MPE at Different Cooling Rates

Sample	Cooling Rate (°C/min)	T_0 (K)	T_p (K)	α_p	α_p' (1/min)
UPE	1	395.18	393.75	0.264	0.468
	5	394.25	391.87	0.279	1.663
	10	393.71	390.63	0.300	2.543
	15	393.35	389.72	0.316	3.191
	20	393	389.14	0.313	3.775
$MPE_{0.23}$	1	397.61	394.97	0.170	0.168
	5	398.35	393.30	0.205	0.755
	10	398.67	392.20	0.227	1.353
	15	398.72	391.60	0.219	1.861
	20	398.85	390.75	0.261	2.353
$MPE_{0.47}$	1	398.99	394.64	0.146	0.148
	5	398.05	392.81	0.193	0.632
	10	398.40	391.56	0.221	1.105
	15	398.12	390.65	0.240	1.519
	20	398.37	389.76	0.276	1.943
$MPE_{0.85}$	1	397.23	394.48	0.154	0.161
	5	397.46	392.48	0.203	0.650
	10	397.83	390.89	0.254	1.116
	15	397.91	390.14	0.243	1.507
	20	397.84	389.07	0.280	1.868
$MPE_{1.68}$	1	397.87	395.11	0.127	0.125
	5	399.68	393.48	0.159	0.573
	10	399.87	392.22	0.199	1.049
	15	399.86	391.14	0.244	1.510
	20	398.82	390.66	0.238	1.907

E_{growth} value of MPE is probably increased with an increase in the MA content. Because the mobility of molecular chains is determinant in crystal growth, the interaction between MA groups probably affects the process of crystal growth more than that of nucleation. The little difference in the value of E between before

TABLE II
Characteristics of DSC Crystallization Exotherms of 85UPE–FC and 85MPE–15FC Composites at Different Cooling Rates

Sample	Cooling Rate (°C/min)	T_0 (K)	T_p (K)	α_p	α_p' (1/min)
85UPE–15FC	1	394.87	393.20	0.270	0.396
	5	393.69	391.02	0.295	1.418
	10	393.06	389.61	0.325	2.202
	15	392.67	388.69	0.322	2.790
	20	392.37	388.18	0.282	3.296
$85MPE_{0.23}$–15FC	1	395.83	393.99	0.168	0.235
	5	395.11	392.17	0.198	0.937
	10	394.68	390.91	0.223	1.556
	15	394.41	390.15	0.213	2.033
	20	394.12	389.08	0.262	2.472
$85MPE_{0.47}$–15FC	1	395.97	393.82	0.113	0.092
	5	395.99	392.16	0.209	0.593
	10	396.19	390.89	0.227	1.063
	15	395.92	389.64	0.268	1.466
	20	396.01	388.94	0.267	1.823
$85MPE_{0.85}$–15FC	1	395.51	393.05	0.125	0.092
	5	395.15	391.15	0.192	0.477
	10	395.10	389.90	0.212	0.887
	15	395.42	388.64	0.249	1.253
	20	395.53	387.47	0.287	1.568
$85MPE_{1.68}$–15FC	1	394.76	389.27	0.263	0.062
	5	394.92	389.98	0.203	0.359
	10	395.43	388.22	0.277	0.726
	15	395.76	387.13	0.307	1.071
	20	395.96	385.99	0.348	1.380

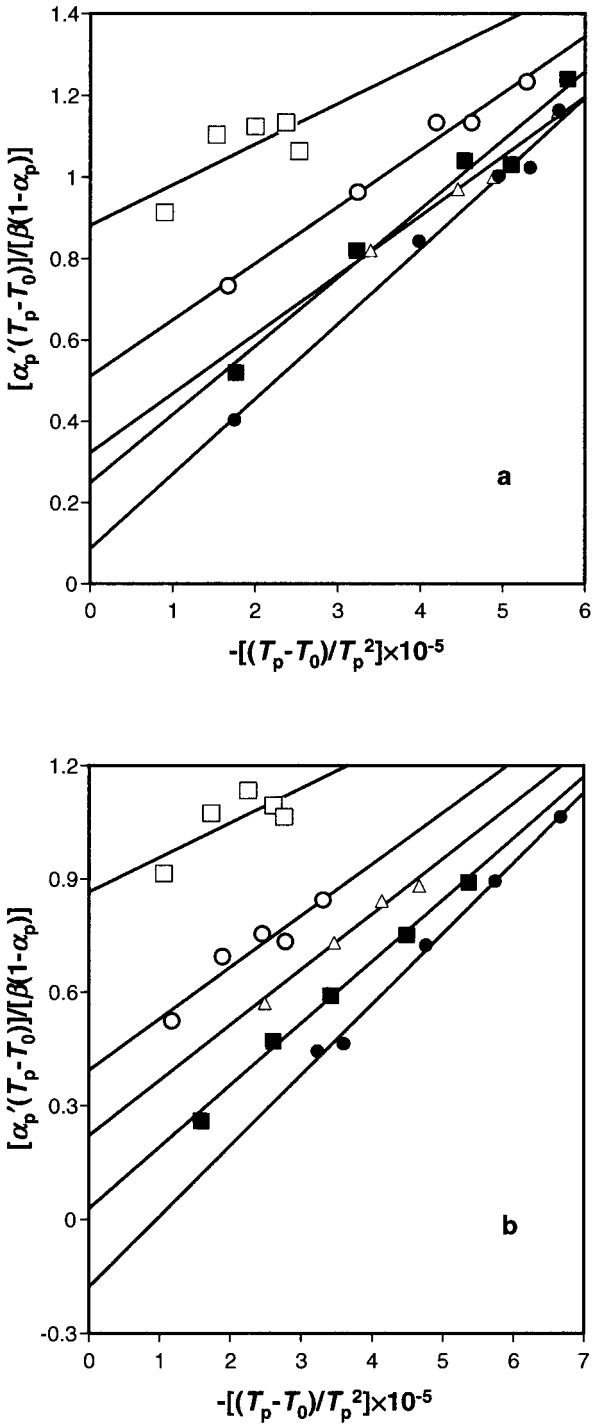

Figure 8 Plots of $[\alpha_p'(T_p - T_0)]/[\beta(1 - \alpha_p)]$ versus $-[(T_p - T_0)/T_p^2]$ for (a) MPE_x and (b) $85MPE_x$–15FC composites, where x = (□) 0, (○) 0.23, (△) 0.47, (■) 0.85, and (●) 1.68.

and after compounding of MPE with FC may be attributable to a negligible interaction of FC with MPE, because the present FC has a particle size of >100 μm and a high crystallinity of 93% as mentioned above.

CONCLUSION

The crystallization and melting of MPE are strongly affected by the MA content. MPE exhibits a higher starting temperature of crystallization, because of the induction of interactions between MA groups for nucleation, and lower melting and crystallization enthalpies, which are due to the intensive irregularity of MPE chains compared to UPE. FC slightly facilitates the nucleation of MPE, but it causes no change in the transition enthalpies of MPE. The kinetics of noniso-

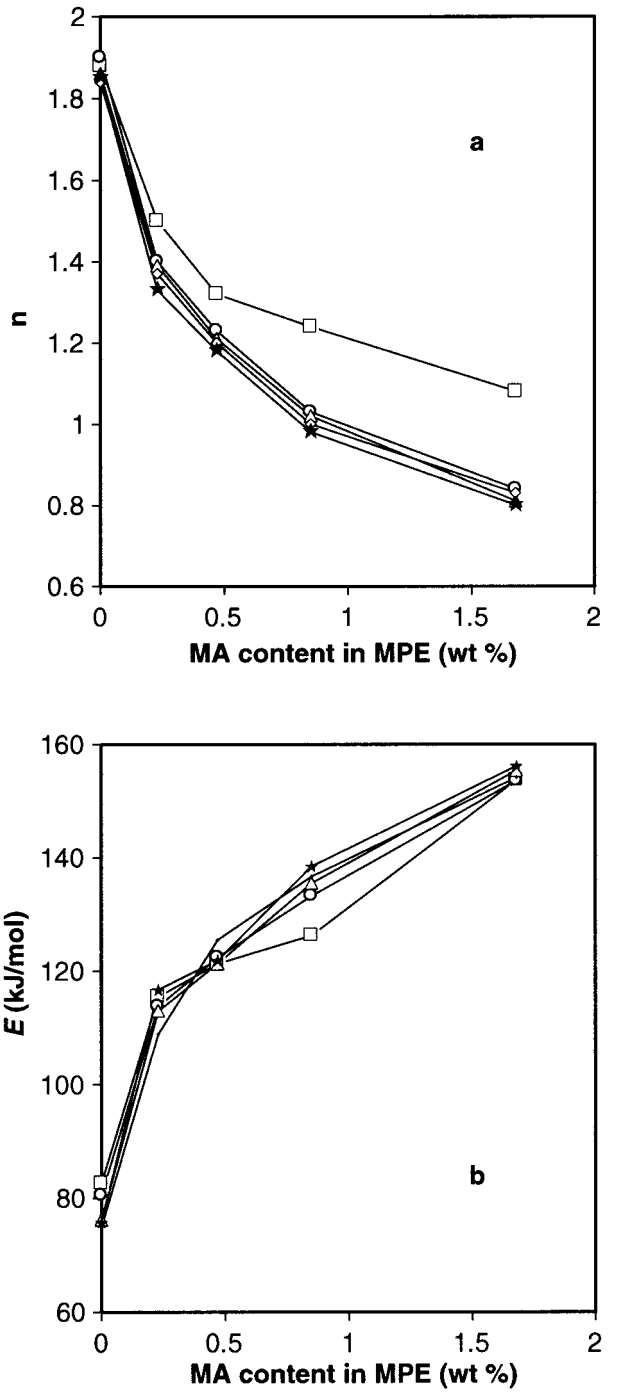

Figure 9 The dependence of the value of (a) n and (b) E on the content of MA groups in MPE for MPE–FC composites with FC contents of (□) 0, (○) 5, (△) 15, (◇) 30, and (★) 60 wt %.

thermal crystallization show that MPE has a larger activation energy and a lower Avrami exponent for crystallization than UPE. The differences in crystallization and melting behaviors between MPE and UPE are probably due to the intensive irregularity and decreased mobility of MPE molecular chains because of the interactions between pendant MA groups.

References

1. Bledzki, A. K.; Gassan, J. Prog Polym Sci 1999, 24, 221.
2. Zhang, F.; Endo, T.; Qiu, W.; Yang, L.; Hirotsu, T. J Appl Polym Sci 2002, 84, 1971.
3. Zhang, F.; Qiu, W.; Yang, L.; Endo, T.; Hirotsu, T. J Mater Chem, 2002, 12, 24.
4. Joly, C.; Kofman, M.; Gauthier, R. J Mol Sci Pure Appl Chem Sci 1997, A33, 1981.
5. Felix, J. M.; Gatenholm, P. J Appl Polym Sci 1991, 42, 609.
6. Karnani, R.; Krishnan, M.; Narayan, R. Polym Eng Sci 1997, 37, 476.
7. Zhang, F.; Kabeya, H.; Kitagawa, R.; Hirotsu, T.; Yamashita, M.; Otsuki, T. Chem Mater 1999, 11, 1952.
8. Heinen, W.; Rosenmoller, C. H.; Wenzel, C. B.; de Groot, H. J. M.; Lugtenburg, J.; van Duin, M. Macromolecules 1996, 29, 1151.
9. Gaylord, N. G.; Mehta, R. J Polym Sci Polym Chem 1988, 26, 1189.
10. Samay, G.; Nagy, T.; White, J. L. J Appl Polym Sci 1995, 56, 1423.
11. De Roover, B.; Sclavons, M.; Carlier, V.; Devaux, J.; Legras, R.; Momatz, A. J Polym Sci Polym Chem 1995, 33, 829.
12. Thompson, M. R.; Tzoganakis, C.; Rempel, G. L. Polymer 1997, 39, 327.
13. Liu, N. C.; Baker, W. E.; Russell, K. E. J Appl Polym Sci 1990, 41, 2285.
14. Yu, J.; He, J. Polymer 2000, 41, 891.
15. Longworth, R.; Vaughan, D. J. Nature 1968, 218, 85.
16. Quiram, D. J.; Register, R. A.; Ryan, A. J. Macromolecules 1998, 31, 1432.
17. Quillin, D. T.; Caulfield, D. F.; Koutsky, J. A. J Appl Polym Sci 1993, 50, 1187.
18. Zhang, F.; Endo, T.; Kitagawa, R.; Kabeya, H.; Hirotsu, T. J Mater Chem 2000, 10, 2666.
19. Endo, T.; Kitagawa, R.; Hirotsu, T.; Hosogawa, J. Kobunshi Ronbunshu 1999, 56, 166.
20. Avrami, M. J Chem Phys 1939, 7, 1103.
21. Avrami, M. J Chem Phys 1940, 8, 212.
22. Ozawa, T. Polymer 1971, 12, 150.
23. Cebe, P. Polym Compos 1988, 9, 271.
24. Liu, T.; Mo, Z.; Wang, S.; Zhang, H. Polym Eng Sci 1997, 37, 568.
25. Lopez, L. G.; Wilkes, G. L. Polymer 1989, 30, 882.
26. Gupta, A. K.; Rana, S. K.; Deopura, B. L. J Appl Polym Sci 1994, 51, 231.
27. Endo, T.; Kitagawa, R.; Zhang, F.; Hirotsu, T.; Hosogawa, J. Chem Lett 1999, 1155.
28. Velasco, I. I.; de Saja, J. A.; Martinez, A. B. J Appl Polym Sci 1996, 61, 125.
29. Hay, J. N.; Perzekop, Z. J. J Polym Sci Polym Phys Ed 1978, 16, 81.
30. Hay, J. N.; Mills, P. J. Polymer 1982, 23, 1380.